Clim. Past Discuss., 7, 2217–2259, 2011
www.clim-past-discuss.net/7/2217/2011/
doi:10.5194/cpd-7-2217-2011
© Author(s) 2011. CC Attribution 3.0 License.

Climate of the Past Discussions

This discussion paper is/has been under review for the journal Climate of the Past (CP). Please refer to the corresponding final paper in CP if available.

Towards orbital dating of the EPICA Dome C ice core using $\delta O_2/N_2$

A. Landais[1,*], G. Dreyfus[1,*,***], E. Capron[1,**], K. Pol[1], M. F. Loutre[2], D. Raynaud[3], V. Y. Lipenkov[4], L. Arnaud[3], V. Masson-Delmotte[1], D. Paillard[1], J. Jouzel[1], and M. Leuenberger[5]**

[1]Institut Pierre-Simon Laplace/Laboratoire des Sciences du Climat et de l'Environnement, UMR8212, CNRS – CEA-CNRS-UVSQ, 91191, Gif-sur-Yvette, France
[2]Université catholique de Louvain, Earth and Life Institute, Georges Lemaître Centre for Earth and Climate Research (TECLIM), Chemin du cyclotron, 2, 1348 Louvain la Neuve, Belgium
[3]Laboratoire de Glaciologie et Géophysique de l'Environnement, CNRS-UJF, 38402 St Martin d'Hères, France
[4]Arctic and Antarctic Research Institute, 38 Bering street, St Petersburg 199397, Russia
[5]Climate and Environmental Physics, Physics Institute, and Oeschger Centre for Climate Change Research, University of Bern, Sidlerstrasse 5, 3012 Bern, Switzerland
[*]now at: American Association for the Advancement of Science (AAAS) Science & Technology Policy Fellow at the National Oceanic and Atmospheric Administration, 1401 Constitution Avenue NW, Washington, DC 20230, USA

**now at: British Antarctic Survey, High Cross, Madingley Road, Cambridge, CB3 0ET, UK
***The two first authors participated equally to this work.

Received: 24 June 2011 – Accepted: 28 June 2011 – Published: 30 June 2011

Correspondence to: A. Landais (amaelle.landais@lsce.ipsl.fr)

Published by Copernicus Publications on behalf of the European Geosciences Union.

Abstract

Based on a composite of several measurement series performed on ice samples stored at −25 °C or −50 °C, we present and discuss the first $\delta O_2/N_2$ record of trapped air from the EPICA Dome C (EDC) ice core covering the period between 300 and 800 ka (thousands of years before present). The samples stored at −25 °C show clear gas loss affecting the precision and mean level of the $\delta O_2/N_2$ record. Two different gas loss corrections are proposed to account for this effect, without altering the spectral properties of the original datasets. Although processes at play remain to be fully understood, previous studies have proposed a link between surface insolation, ice grain properties at close-off and $\delta O_2/N_2$ in air bubbles, from which an orbitally tuned chronologies of the Vostok and Dome Fuji ice core records have been derived over the last four climatic cycles. Here, we show that limitations caused by data quality and resolution, data filtering and uncertainties in the orbital tuning target limit the precision of this tuning method for EDC to at least 2.5 kyrs (thousands of years). Moreover, our extended record includes two periods of low eccentricity. During these intervals (around 400 ka and 750 ka), the matching between $\delta O_2/N_2$ and the different insolation curves is ambiguous because some local insolation maxima cannot be identified in the $\delta O_2/N_2$ record (and vice versa). Recognizing these limitations, we restrict the use of our $\delta O_2/N_2$ record to show that the EDC3 age scale is generally correct within its published uncertainty (6 kyrs) over the 300–800 ka period. We illustrate the uncertainties associated with data quality, filtering and tuning target for periods of low eccentricity by highlighting the difficulty to constrain the duration of Marine Isotopic Stage 11 based on the EDC $\delta O_2/N_2$ information.

1 Introduction

While ice core records offer a wealth of paleoclimatic and paleoenvironmental information, uncertainties associated with ice core dating limit their contribution to the

CC BY

understanding of past climate dynamics. Absolute age scales have been constructed for Greenland ice cores thanks to layer counting in sites offering sufficient accumulation rates (GRIP, GISP2, NorthGRIP (Rasmussen et al., 2006; Svensson et al., 2006; 2008)), allowing to build the GICC05 Greenland age scale currently spanning the past 60 ka (thousand of years before present). While layer counting is not possible for deep Antarctic ice cores obtained in low accumulation areas, the transfer of the GICC05 age scale (using gas synchronization methods, (e.g. Blunier et al., 2007)) to Antarctic records allows to partly circumvent this difficulty for the past 60 ka. Absolute time markers are generally lacking for these long Antarctic records, now extending up to 800 ka, with the exception of promising studies using the Ar/Ar and U/Th dating tools (Dunbar et al., 2008; Aciego et al., 2010) and the links between ^{10}Be peaks and well dated magnetic events (Raisbeck et al., 2007, 2008). As a result, dating of the deepeest part of these Antarctic cores is largely based on various approaches combining an ice flow model with orbital tuning. Classically, orbital tuning assumes that northern hemisphere summer insolation drives large climate transitions (e.g., Milankovitch, 1941), and has long been used for dating paleoclimatic records, especially marine ones (e.g. Martinson et al., 1987).

As for Antarctic ice cores, two different orbital dating approaches, both initially developed by Bender et al. (1994) and Bender (2002), are now commonly used. First, long records of δ^{18}O of atmospheric O_2 ($\delta^{18}O_{atm}$) have revealed that this parameter is highly correlated with variations in the precession band with a lag of about 5-6 kyrs (thousands of years) (Bender et al., 1994; Petit et al., 1999; Dreyfus et al., 2007). Studies have linked variations in precession to $\delta^{18}O_{atm}$ through changes in low latitude water cycle and biospheric productivity (Malaizé et al., 1999). The significant time delay between changes in precession and changes in $\delta^{18}O_{atm}$ has been attributed to a combination of the 1000–2000 yr residence time of O_2 in the atmosphere (Bender et al., 1994; Hoffmann et al., 2004) and to the numerous and complex processes linking the isotopic composition of seawater to atmospheric oxygen via the dynamic response of the tropical water cycle to precession forcing and the associated variations in

CPD
7, 2217–2259, 2011

CC BY

terrestrial and oceanic biospheres (Landais et al., 2010, and references therein). This superposition of processes also suggests that lags may vary with time (Jouzel et al., 2002; Leuenberger, 1997). As a consequence, the $\delta^{18}O_{atm}$ record from long ice cores can be used to constrain ice core chronologies (e.g., Petit et al., 1999; Shackleton, 2000), but with a large associated uncertainty (6 kyrs) (Petit et al., 1999; Dreyfus et al., 2007). In parallel, the link between precession, low latitude hydrology, and atmospheric methane concentration (Chappellaz et al., 1993) has been used to propose an orbital age scale for Vostok (Ruddimann et al., 2003). However, past methane variations exhibit a strong impact of obliquity (Loulergue et al., 2008), and a weaker correlation with precession than $\delta^{18}O_{atm}$ (Schmidt et al., 2004; Landais et al., 2010) hence limiting this approach.

Second, Bender (2002) has proposed that the elemental ratio $\delta O_2/N_2$ in the trapped air could be used as a new orbital tuning tool. Indeed, $\delta O_2/N_2$ measurements in the firn near the pore close-off depth (about 100 m below the ice-sheet surface, i.e. where unconsolidated snow is compressed to the density of ice) have revealed that the trapping process is associated with a relative loss of O_2 with respect to N_2 (Battle et al., 1996; Severinghaus and Battle, 2006; Huber et al., 2006). Between 160 and 400 ka, the $\delta O_2/N_2$ record of the Vostok ice core displays variations similar to those of the local 21 December insolation (78° S). From these two observations, Bender (2002) formulated the hypothesis that local Antarctic summer insolation influences near-surface snow metamorphism and that this signature is preserved during the firnification process down to the pore close-off depth, where it modulates the loss of O_2. From this hypothesis, they proposed to use of $\delta O_2/N_2$ for dating purposes.

Despite a limited understanding of the physical mechanisms linking local 21 December insolation and $\delta O_2/N_2$ variations in polar ice cores, this approach has been used by Kawamura et al. (2007) and Suwa and Bender (2008a) to propose an orbital dating of the Dome F and Vostok ice cores respectively back to 360 and 400 ka. The validity of the link with local insolation has been supported by a similar correspondence observed on the Greenland GISP2 ice core (Suwa and Bender, 2008b). Using their high quality $\delta O_2/N_2$ record on the Dome F ice core and comparison with radiometric dating obtained on speleothem records, Kawamura et al. (2007) estimated the dating uncertainty to be as low as 0.8–2.9 kyrs. Moreover, it was suggested that, combined with an inverse glaciological modeling approach, the dating uncertainty could be pinched down to 1 kyr (Parrenin et al., 2007).

Up to now, the oldest ice core climatic and greenhouse gases records have been obtained from the EPICA Dome C (EDC) ice core that covers the last 800 ka (Jouzel et al., 2007; Lüthi et al., 2008; Loulergue et al., 2008). The state of the art dating of the EDC ice core (EDC3 chronology) has been described in Parrenin et al. (2007): it is based on ice flow modeling using an inverse method constrained by available age markers. These age markers include reference horizons such as volcanic horizons (Mt Berlin eruption, 92.5 ka (Dunbar et al., 2008)) and peaks in ^{10}Be flux (i.e. Laschamp event, 41.2 ka (Yiou et al., 1997; Raisbeck et al., 2008)). Other tie points have been introduced based on the comparison of the ice core records with records of other well dated archives: as an example, the abrupt methane increase at Termination 2 was assumed to be synchronous (within 2 kyrs) with the abrupt $\delta^{18}O$ of calcite (speleothem) shift recorded in Chinese (Yuan et al., 2004) and Levantine (Bar-Mathews et al., 2003) regions at around 130.1 ka. For the last 42 ka, the EDC3 age scale was synchronized with the layer-counted Greenland GICC05 chronology (Svensson et al., 2008) with a recent improvement by Lemieux-Dudon et al. (2010). For ice older than the last interglacial period, tie points are exclusively derived from orbital tuning. In addition to 37 $\delta^{18}O_{atm}$ tie points used between 400 and 800 ka, additional orbital information was derived from local insolation changes imprinted in the record of total air content in polar ice. Raynaud and colleagues (2007) indeed showed that the majority of the variance in total air content in the EDC ice core can be explained by the variations of an integrated summer insolation parameter (i.e. summation of the daily insolation over a certain threshold for a given latitude) that has a dominant obliquity component. This marker was therefore suggested as another tool for orbital dating of ice core records. Ten such "air content" tie points have been used between 71 and 431 ka for EDC3, assuming a 4 kyrs uncertainty to account for scatter in the raw data and the uncertainty due to the choice of the integrated summer insolation target (threshold value for daily insolation). The overall uncertainty attached to the EDC3 time-scale is estimated to 6 kyrs from 130 ka down to the bottom of the record. As a result, the accuracy of event durations is as large as 40 % between 400 and 800 ka (i.e. over the period mainly constrained by $\delta^{18}O_{atm}$ orbital tuning) (Parrenin et al., 2007).

In this article, we present the first records of $\delta O_2/N_2$ measured on the EDC ice core between 800 and 300 ka. This record is of special interest since (1) no $\delta O_2/N_2$ data were used for constraining the EDC3 age scale, and (2) no $\delta O_2/N_2$ data have so far been published prior to 410 ka. Our record includes two periods of minimum eccentricity, centered at around 400 ka and around 750 ka, characterized by a minimum influence of precession variations on insolation (Loutre and Berger, 2003). This contrasts with the relatively large eccentricity context for the time interval between 50 and 360 ka, where previous $\delta O_2/N_2$ records were obtained. Our $\delta O_2/N_2$ record is therefore used for examining (1) the feasibility of orbital dating (in particular with $\delta O_2/N_2$) at times of low eccentricity, and (2) the validity of the EDC3 age scale between 300 and 800 ka with respect to the $\delta O_2/N_2$ constraints.

We first examine the analytical methods used to perform the measurements, as well as discuss the effects of gas loss associated with ice storage on the integrity of the $\delta O_2/N_2$ record and the necessary corrections. The spectral properties of the resulting composite EDC $\delta O_2/N_2$ curve are then analyzed with respect to the orbital forcing. The local insolation influence on this EDC signal is compared with previous studies on the Vostok and Dome F ice cores (Bender, 2002; Kawamura et al., 2007; Suwa and Bender, 2008). The uncertainties and limitations attached to the use of $\delta O_2/N_2$ as a dating tool for the EDC ice core between 300 and 800 ka are quantified; we combine $\delta O_2/N_2$ and $\delta^{18}O_{atm}$ to assess the uncertainty of the EDC3 age scale. With a specific focus on Marine Isotopic Stage 11 (around 400 ka), we finish by discussing the current limits of the use of $\delta O_2/N_2$ for this part of the EDC ice core.

CPD
7, 2217–2259, 2011

CC BY

2 Methods

2.1 Technique used at LSCE for obtaining the EDC $\delta O_2/N_2$ record

The technique used at LSCE for extracting the air trapped in ice core samples is based on melting and refreezing ice samples as first developed by Sowers et al. (1989) and detailed in Landais et al. (2003). For each depth, two adjacent ice samples covering the same depth interval are cut from the ice core. Approximately 3–5 mm of the outer ice is shaved off each face to yield two 10 g ice samples. The samples are placed in pre-cooled glass flasks with glass/metal transitions to Conflat flange tops. The flasks are connected to a vacuum manifold using gold-plated copper gaskets. The manifold is equipped with a Pfeiffer-Balzar turbo molecular pump, two pressure gauges (Baratron, Pirani), manual Nupro valves, and 6 ports. Typically, we process 6 samples per day with this method in two shifts of three. Following a leak test, the ambient air surrounding the ice samples is evacuated using a turbo-molecular pump for 35–40 min while ice is kept frozen by immersing the flask in a −20 °C ethanol bath. The flask is then isolated using a manual Nupro valve, and the ice is allowed to melt at room temperature. Once the samples are completely melted, we begin refreezing the first sample. Since only one sample can be cryogenically transferred at a time, the samples are refrozen sequentially. Refreezing is accomplished using a 10 cm long copper cold finger with flat top plate placed in contact with the bottom of the sample flask. Only the bottom 3 cm of the cold finger are initially immersed in liquid nitrogen. Heat transfer is facilitated by adding alcohol to the top plate in contact with the flask bottom. This arrangement allows the melt water to refreeze slowly from the bottom, minimizing the capture of dissolved gases. Cracking of the ice signals refreezing is complete, at which time we completely immerse the cold finger in liquid N_2. In order to remove residual water vapor from the headspace, we heat the metal flange connection with a heat gun for 2.5 min, then maintain the cold flinger maximally immersed in liquid N_2 for an additional 10 min, a procedure ensuring that the sample flask is never in direct contact with liquid N_2. The headspace gases are then cryogenically transferred into a quarter inch steel tube plunged into liquid He for 6 min. The gases in the stainless steel tube are allowed to come to room temperature and equilibrate for a minimum of 40 min before being introduced into the mass spectrometer for isotopic and elemental analysis using a dual inlet system.

The measurements of $\delta O_2/N_2$ on the EDC ice core were performed on two different mass spectrometers. The first series (Table 1, Fig. 1) was obtained on a 4-collector Finnigan MAT 252. On this mass spectrometer, the masses (m/z) 32 (O_2) and 28 (N_2) could not be measured simultaneously so that $\delta O_2/N_2$ was measured by interfering masses (jumping from one mass to the other). The second, third and fourth measurement series (Table 1, Fig. 1) were measured on a 10-collector Thermo Delta V Plus that permitted simultaneous acquisition of m/z 32 and 28. A careful inter-comparison of the performances of the two mass spectrometers using air standard and firn air on the two instruments showed no significant offsets (Dreyfus, 2008).

The method for $\delta O_2/N_2$ measurements at LSCE is similar to the one used for obtaining the Vostok $\delta O_2/N_2$ record (Sowers et al., 1998; Bender, 2002). However, it significantly differs from the one used for the Dome F $\delta O_2/N_2$ record (Kawamura et al., 2007) which requires a much larger ice sample (~ 200 g instead of 10 g) and is based on a gas extraction with no refreezing (Kawamura et al., 2003). No inter-calibration of these different methods has yet been conducted.

2.2 EDC raw data

The measurements have been performed on clathrate ice below 2400 m depth well below the bubble – clathrate transition zone where positive $\delta O_2/N_2$ values have been observed in other records. This effect is due to O_2 being more easily dissolved in ice as gas hydrates than N_2 so that after coring, N_2 (from bubbles) is preferentially lost relative to O_2 (from clathrates) in this zone (Bender, 2002; Ikeda-Fukazawa et al., 2005). The complete record is a composite of four different series of measurements from ice with different storage histories (Table 1, Fig. 1). All data have been corrected

CPD
7, 2217–2259, 2011

Towards orbital dating of the EPICA Dome C ice core

A. Landais et al.

Discussion Paper | Discussion Paper | Discussion Paper | Discussion Paper |

for gravitational fractionation as follows:

$$\delta O_2/N_2 = \delta O_2/N_{2,\text{raw}} - 4 \times \delta^{15}N \quad (1)$$

For all series, each sample value corresponds to the average of at least two replicate samples analyzed at each depth level. We then calculated the pooled standard deviation as:

$$\sigma_p = \sqrt{\frac{\sum((n_i - 1)\sigma_i^2)}{\sum(n_i - 1)}} \quad (2)$$

where n_i and σ_i are respectively the sample size and the standard deviation of the i^{th} sample. Over the whole set of measurements, σ_p is equal to 1.5‰.

As expected from the inter-comparison between the two mass spectrometers, no shift between the mean values appears between the 1st and the 2nd series. The oldest values (700–800 ka) obtained in series 2 are associated with a large scatter of the $\delta O_2/N_2$ data between neighboring and replicate samples. For two of these depth levels, $\delta O_2/N_2$ reaches extremely low values (lower than 40‰) with an associated standard deviation of 10‰ (Fig. 1). These ice samples are likely affected by significant gas loss after ice coring that favors the loss of the smaller molecule O_2 with respect to the larger molecule of N_2 (Huber et al., 2006).

On the contrary, samples from series 3 (stored at −50 °C instead of at -25°C as for series 1 and 2) are associated with a very low pooled standard deviation (0.32‰). This shows that high precision $\delta O_2/N_2$ measurements on EDC ice are possible with our experimental set-up if the ice is stored at a very low temperature. Moreover, samples from series 4, also stored at −50 °C, show a significantly lower scattering than the measurements performed over the same depth range from series 2 from ice stored at −25 °C. This again confirms the quality of $\delta O_2/N_2$ record from EDC ice samples stored at −50 °C. Still, the uncertainty associated with series 4 is larger than the one associated with series 3 despite the fact that the samples were stored under the same conditions. This may be related to the ice history, with warmer temperatures encountered near Dome C bedrock (above −10 °C), to the difficulties to extract the deepest ice cores, with increased fragmentation of the cores (short fractured cores of ∼20 cm using ethanol as a drilling liquid), or to a change in ice crystal structure at high depths (Pol et al., 2010; Durand et al., 2010).

3 Gas loss correction and construction of a composite curve

3.1 Principle of gas loss from air bubbles

Bender et al. (1995) showed anomalously low O_2/N_2 and Ar/N_2 ratios in air extracted from ice cores compared to atmospheric air. This effect was initially attributed to gas loss during coring and storage, with the smallest molecules (O_2, Ar) being more easily lost that the larger ones (N_2). Ikeda-Fukazawa et al. (2005) observed a drift in the O_2/N_2 ratio correlated with the storage duration. Two mechanisms have been proposed to explain this size dependent effect: diffusion through the ice lattice by breaking of hydrogen bonds (Ikeda-Fukazawa et al., 2005) or diffusion through small channels in the ice with a threshold dimension of 3.6 Å (i.e. molecules with a diameter larger than 3.6 Å, like N_2, will not escape from the bubbles) (Huber et al., 2006).

For the Dome F ice, Kawamura et al. (2007) found that $\delta O_2/N_2$ decreased by 6.6 ‰ per year of storage at −25 °C, and used this relationship to apply a gas loss correction. While the exact storage temperature histories of our samples are less well known, we observe significant shifts in $\delta O_2/N_2$ levels between samples stored 1–2 yr at −25 °C (series 1 and 2) and samples stored at EDC (−50 °C) and maintained at this temperature during transport and storage (series 3 and 4) as depicted above.

3.2 Corrections

In order to remove outliers, we excluded all the measurements at depth levels where the $\delta O_2/N_2$ standard deviation associated with replicates is larger than 3 ‰ (Fig. 1).

This rejects less than 16 % of the data (mainly over the deepest part of series 2, see details in Table 1) and results in a pooled standard deviation of 0.9 ‰. This is very comparable to the pooled standard deviation obtained on the $\delta O_2/N_2$ records of the Vostok and Dome F ice cores after gas loss correction and removal of 15 to 20 % of outliers (Bender, 2002; Kawamura et al., 2007; Suwa and Bender, 2008a).

The second correction accounts for a systematic bias in the measurements when ice is stored at −25 °C instead of −50 °C. It is based on the following observations: (a) there is no obvious shift between series 1 (measured in 2004–2005) and 2 (measured in 2006–2007); (b) after an homogenization of series 1, 2 and 3 through a linear interpolation every 1 kyr between 380 and 480 ka, we found an average offset between series 1 and 2 on the one hand and series 3 on the other hand of 6.43 ‰. We thus decided to shift all the $\delta O_2/N_2$ values of series 1 and 2 by adding 6.43 ‰. We call this "gas loss correction 1".

This correction is subject to discussion. In particular, it leads to a significant decrease in $\delta O_2/N_2$ with time: the mean $\delta O_2/N_2$ level before 480 ka is less depleted than the mean $\delta O_2/N_2$ level after 380 ka (Fig. 2); the variance of the whole record after the rejection of outliers and "gas loss correction 1" is about 13 ‰. We therefore propose an alternate correction, "gas correction 2". This second correction aims to homogenize (1) the mean level of $\delta O_2/N_2$ between series 2 and series 4 around 700–750 ka, (2) the mean level of $\delta O_2/N_2$ between series 1, 2 and series 3 around 430–480 ka and (3) the mean level of $\delta O_2/N_2$ between series 1 and series 3 around 380–430 ka. In order to fulfill requirements (1) and (2), a simple solution is to add 2.5 ‰ to the $\delta O_2/N_2$ of series 1 and 2 between 430 and 700 ka. Then, in order to fulfill requirement (3), one possible solution (albeit not the only one) is to apply the following correction to series 1 and 2 between 300 and 430 ka:

$$\delta O_2/N_2\_corr = \delta O_2/N_2\_raw + 2.5 - 0.035 \times (t - 500) \quad (3)$$

where $\delta O_2/N_2$_corr is the corrected $\delta O_2/N_2$, $\delta O_2/N_2$_raw is the original $\delta O_2/N_2$ measurements from series 1 and 2 and t is the age of the $\delta O_2/N_2$ data point in ka.

CPD
7, 2217–2259, 2011
Towards orbital dating of the EPICA Dome C ice core
A. Landais et al.

The final variance of the $\delta O_2/N_2$ record after outlier rejection and "gas loss correction 2" is less than 9‰ which is comparable with the variance of the Dome F and Vostok $\delta O_2/N_2$ records.

3.3 Reconstructed curve from EDC $\delta O_2/N_2$

We now construct a composite EDC $\delta O_2/N_2$ record over the period 300–800 ka as follows:

- when series 1 and 2 overlap with series 3 and 4, we only keep the measurements from series 3 and 4.

- we use the two gas loss corrections (outlier correction and gas loss correction) described in the previous paragraph for series 1 and 2 on the remaining periods.

Because we have two alternative "gas loss corrections", we produce two different composite curves, hereafter curves 1 and 2 (Fig. 2). This provides a means of estimating the effect of our subjective gas loss corrections on the final $\delta O_2/N_2$ record. An obvious difference between the two composite curves is the temporal evolution of $\delta O_2/N_2$ with time. While curve 1 shows a long term decrease of $\delta O_2/N_2$ of −0.014‰ per kyr, its value is only of −0.008‰ per kyr for curve 2 (Fig. 2). Even if our gas loss corrections are somehow empirical, the general long term evolution of $\delta O_2/N_2$ with time cannot be cancelled out by any gas loss correction. Indeed, this evolution is due to the fact that the average $\delta O_2/N_2$ is higher on series 4 than on series 3 and none of these series should be affected by gas loss (storage at −50 °C) so that no correction have been applied to them.

For Vostok, a decrease of −0.013‰ per kyr has been observed between 150 and 400 ka (Bender, 2002; Suwa and Bender, 2008a) while Dome F data (Kawamura et al. 2007) show a smaller negative temporal trend (decrease of −0.006‰ per kyr). Given that various gas loss corrections are applied to these different data sets, we cannot assess the origin of this trend, i.e. natural long term $\delta O_2/N_2$ variability, gas loss effect or pore close-off effect.

3.4 Comparison with previous $\delta O_2/N_2$ records

Figure 3 displays the comparison between the two composite curves obtained from our EDC $\delta O_2/N_2$ data and the previous $\delta O_2/N_2$ records from Dome F (Kawamura et al., 2007) and Vostok (Bender et al., 2002; Suwa and Bender, 2008a). Because of the different time periods covered by the different ice cores, the comparison is restricted to the period 300–340 ka for Dome F and EDC and 300–410 ka for Vostok and EDC. The general evolutions of the $\delta O_2/N_2$ records are in agreement except for two features. First, the large peak observed around 400 ka on the EDC record appears as a double peak in the Vostok record. We have confidence in the quality and resolution of our measurements over this period because they were performed on ice stored at −50°C with a pooled standard deviation of 0.32‰ and a mean age resolution of 1.5 kyr. Second, the Dome F data are on average less depleted than the Vostok and EDC data. This could be due to differences in gas loss effect resulting from different stress experienced by each core after coring. However, we have applied our empirical gas loss corrections to the EDC data over the period 300–340 ka, so a future comparison on samples minimally affected by gas loss would be more useful to evaluating such an effect.

4 Spectral properties and link with orbital frequency

4.1 Spectral analysis

The initial $\delta O_2/N_2$ data set on the EDC3 age scale over the period 300 to 800 ka is associated with a minimum, average and maximum sampling step of 1, 2.5 and 6 kyrs (the latter only in one extreme case) respectively. The data are first interpolated at a constant time step. The Multi-Taper Method, producing a spectrum in amplitude, is then used to identify the major spectral components of the $\delta O_2/N_2$. We have checked that the results are robust with respect to the spectral analysis method as well as with

CC BY

respect to the resampling. Indeed, the same spectral components were obtained using the Blackman Tukey or Classical FFT (Fast Fourier transform) periodogram methods albeit with different amplitudes. Reinterpolating the data at steps of 2 or 3 kyrs does not yield significantly different results. These analyses were performed with the Analyseries software (Paillard et al., 1996).

For the two corrected curves, we observe the same significant frequency peaks (Fig. 4a). Two large peaks coincide with the frequencies of precession (periods of 23 kyrs and 19 kyrs). A spectral peak at 41 kyrs is associated with obliquity (less prominent with the Blackman-Tuckey method) and a significant peak at 28 kyrs is identified (however not visible with the Blackman Tuckey method).

Our results show the same general pattern as the spectral analysis of the $\delta O_2/N_2$ records of Vostok over the period 150–400 ka (Bender, 2002) and of Dome F between 82 and 360 ka (Kawamura et al., 2007) with a large peak corresponding to a period of 23 kyrs and a smaller one corresponding to a period of 41 kyrs. We note that neither Vostok nor Dome F $\delta O_2/N_2$ records exhibit a shoulder at 19 kyrs.

As already depicted in previous studies, the $\delta O_2/N_2$ power spectrum resembles that of local insolation, more precisely the insolation received at the 21 December at Dome C site, with the dominance of precession and obliquity (Fig. 4b). It should be noted that the 19-kyr peak, corresponding to precession frequency, is present both in the spectrum of $\delta O_2/N_2$ from our record between 300 and 800 ka and in local 21 December or December insolation spectra over the same period. In contrast, it is less obvious from both the spectrum of $\delta O_2/N_2$ and in the summer insolation spectrum over the last 400 ka (Bender, 2002; Suwa and Bender, 2008a; Kawamura et al., 2007).

4.2 Impact of data filtering

Filtering the $\delta O_2/N_2$ record reveals the strong correlation with orbital forcing. Following previous studies (Kawamura et al., 2007; Suwa and Bender, 2008a), we performed a data re-sampling with a step of 1 kyr and the resampled series were band pass filtered based on a fast Fourrier transform (FFT) using a piecewise linear window with sharp

Discussion Paper | Discussion Paper | Discussion Paper | Discussion Paper |

CPD

7, 2217–2259, 2011

Towards orbital dating of the EPICA Dome C ice core

A. Landais et al.

Title Page
Abstract Introduction
Conclusions References
Tables Figures
◄◄ ►►
◄ ►
Back Close
Full Screen / Esc

Printer-friendly Version

Interactive Discussion

slopes at the edges (<10–5 $kyrs^{-1}$) (Analyseries software; Paillard et al., 1996). In order to study the link between $\delta O_2/N_2$ and local summer insolation, it is essential that the precession and obliquity frequencies are preserved. Therefore, we choose two different ranges of filtering frequencies corresponding to the following periods: 15–100 kyrs and 15–60 kyrs (Fig. 5). These filters have been selected because none of them affects the position of the peaks of the local insolation curves, similarly to digital filter described in Kawamura et al. (2007) based on finite duration impulse response. They were applied on both composite curves giving results similar to the digital filter of Kawamura et al. (2007) (Fig. 5). While none of these filters affects the position of the peaks of the insolation curves by more than 0.15 kyrs, they slightly influence the timing of the EDC $\delta O_2/N_2$ extrema (Fig. 5), which can have important consequences when matching $\delta O_2/N_2$ record with insolation curves.

The time-delays between the filtered $\delta O_2/N_2$ records using both different filtering ranges have been quantified using the cross-wavelet transform technique (Mallat, 1998; Torrence and Compo, 1999) as follows. The cross-wavelet spectrum of two series, computed from the continuous wavelet transform of each series, provides an estimate of the local phase difference between the two series for each point of the time-frequency space. Its integration over a frequency interval allows the computation of the instantaneous time lag between the two series in the corresponding frequency band (Mélice and Servain, 2003). With this method, the time-delays between the filtered $\delta O_2/N_2$ obtained with the different filtering ranges is of a few centuries (Fig. 5), with the exception of the period 380–450 ka where the shifts can reach 1 kyr. There are two main causes for the time shifts detected by the different filtering methods: the resolution of the data and the ratio between signal and noise. Tests with resolution ranging from 1 to 5 kyrs have shown that peaks can be shifted by a maximum of ±300 yrs over the period 300 to 450 ka. Monte-Carlo tests on white noise added to our composite $\delta O_2/N_2$ curve have produced peak displacements of up to ±1.3 kyr (2 σ), in particular over the period from 300 to 400 ka. Shifts in peak position from filtering are largest over the period 340–360 ka (small signal and poor resolution), 360–450 ka

CC BY

(small signal) and between 610 and 680 ka (poor resolution). In the following, we consider the $\delta O_2/N_2$ record filtered between 15 and 100 kyrs. Because of the time shift in the $\delta O_2/N_2$ extrema discussed above, their position is associated with an uncertainty of 1 kyr between 380 and 450 ka, and 0.5 kyr elsewhere.

Finally, we can get a qualitative sense of the validity of the filtered curve by comparing it directly with the original data (Fig. 5). As discussed above, this comparison reveals two periods, i.e. between 610 and 680 ka and between 340 and 360 ka, with relatively sparse $\delta O_2/N_2$ coverage and small $\delta O_2/N_2$ variations making identification and correlation of extrema with the filtered curve ambiguous at best. For this reason, we refrain from drawing strong conclusions on the chronology over this period.

4.3 Link with local summer insolation

The previous studies using $\delta O_2/N_2$ (Bender, 2002; Kawamura et al., 2007; Suwa and Bender, 2008a, 2008b) have compared the $\delta O_2/N_2$ records over the last 400 ka with 21 December insolation or monthly (December) mean insolation at the latitude of each ice core, which display only minor differences. Based on the assumption that the phase lag between $\delta O_2/N_2$ and 21 December insolation is nil as suggested by the Vostok data (Bender, 2002), the new dating of Vostok, Dome F and GISP2 were constructed by matching the peaks of the filtered $\delta O_2/N_2$ curve and of either December (Suwa and Bender, 2008a, 2008b) or 21 December insolation (Kawamura et al., 2007).

We have however several reasons for raising doubts on the fact that $\delta O_2/N_2$ in the EDC ice core is solely dependent on 21 December or December insolation (which have very similar spectra properties). While Kawamura et al. (2007) have shown a strong link between 21 December insolation and the seasonal maximum of Dome F surface temperature (with no lag), we find a different timing between surface air and snow temperature at Dome C with a lag of 15–20 days between the maximum of insolation (21 December) and the temperature maximum (Fig. 6).

The mechanisms linking surface temperature, snow metamorphism and hence $\delta O_2/N_2$ are only partially understood. In particular, $\delta O_2/N_2$ does not display any link

CC BY

with the largest temperature changes observed during terminations (Kawamura et al., 2007). We note that, using a simple model describing the evolution of temperature gradient metamorphism affecting the snow structure with respect to local insolation, Hutterli et al. (2010) proposed that the variations of accumulation compensate those of temperature during terminations. However, they also suggest that significant shifts by several kyrs can exist between snow metamorphism and 21 December local insolation. Whether or not $\delta O_2/N_2$ is systematically linked with 21 December local insolation whatever the climatic conditions at the site and the orbital context, can thus still be considered as an open question.

To further explore this question, we have chosen to examine the link between our $\delta O_2/N_2$ record and local insolation (75° S) using two different reference curves: the 21 December insolation (as in previous studies) and the mean insolation received from the 21 December until the 21 March (hereafter called 21 December–21 March local insolation). Insolation is computed with Analyseries software (Paillard et al., 1996) according to Laskar (2004) astronomical solution. Values are computed with a time step of 1 kyr and then filtered to keep only the periodicities between 15 and 100 kyrs (Fig. 7). We thus end with two insolation curves, the 21 December insolation (classical approach) and 21 December–21 March insolation (alternative choice) that show significant differences both in the amplitude and in the phasing of the minima and maxima (Fig. 6). Here the dates are defined according to the "regular" calendar. However, they could have been defined according to the astronomical calendar. In that case, the length of the chosen interval (e.g. astronomical austral summer) varies in time with the orbital configuration (i.e. Berger and Loutre, 1994; Huybers and Denton, 2008). Moreover, the true solar longitude (i.e. astronomical date) corresponding to the 21 December also varies in time, according to precession. Today, the seasonal cycle of modern central East Antarctic surface air temperature peaks in December-January: so that the 21 December–21 March local insolation curve is a rather unlikely tuning target for capturing the local temperature maximum. Again, our sole objective in using a different insolation target is to test if whether or not, the EDC $\delta O_2/N_2$ depends on local

CPD
7, 2217–2259, 2011

Towards orbital dating of the EPICA Dome C ice core

A. Landais et al.

cc BY

21 December insolation only.

The comparison between our $\delta O_2/N_2$ filtered data (curves 1 and 2) and the two different insolation targets are first explored through a correlation calculation enabling a relative temporal shifting between the series (cross correlation function of Analyseries (Paillard, 1996)). Considering the whole record, we observe the maximum R^2 when comparing our filtered $\delta O_2/N_2$ curves with the insolation at 75° S on the 21 December ($R^2 = 0.51$ for the two corrections with a shift between the two series of 2 kyrs), slightly better than with the 21 December–21 March insolation at 75° S ($R^2 = 0.45$–0.48 with no temporal shift depending on the gas loss correction). Note that the R^2 coefficients are also influenced by the filtering of our data: using unfiltered data leads to a R^2 of ~0.18 between $\delta O_2/N_2$ and 21 December–21 March insolation and ~0.21 between $\delta O_2/N_2$ and insolation at 75° S on the 21 December.

This simple correlation analysis supports the classical use of the 21 December local insolation as a general target curve for $\delta O_2/N_2$ for the period 300–800 ka. However, the relatively high correlation between $\delta O_2/N_2$ and 21 December insolation at 75° S is not constant through time over our period of interest. In particular, if we focus on the period between 306 and 500 ka, the filtered $\delta O_2/N_2$ seems better tied to the 21 December–21 March insolation ($R^2 = 0.44$–0.46 depending on the gas loss correction) than to the insolation the 21 December ($R^2 = 0.37$–0.42 depending on the gas loss correction). These differences are clearly visible in Fig. 7: while there is a clear correspondence between the relative amplitude of the peaks of the $\delta O_2/N_2$ record and those of the 21 December local insolation between 500 and 800 ka, $\delta O_2/N_2$ relative peak amplitudes are, between 300 and 500 ka, more similar to the relative amplitudes of the smooth peak of the 21 December–21 March local insolation. Such surprising similarity should be verified on a new set of data but we rule out that it is an artifact of data quality because series 3 (380 and 480 ka) is of good quality.

Next, we complement this correlation analysis with a time delay analysis (Fig. 7). We note several features of this phase analysis. First, we observe the same evolution of time delays with respect to each of the insolation curves: the time delays exhibit four

CC BY

maxima at ~450, ~550, ~650 and ~750 ka. Second, we observe that the average time delay is 0 ka when comparing $\delta O_2/N_2$ with the summer daily mean irradiance, while it reaches 2 kyrs when comparing $\delta O_2/N_2$ with insolation the 21 December. This results from the almost constant time delay of 2 kyrs between local insolation the 21 December and 21 December–21 March local insolation. Note that this time delay analysis does not depend on the gas loss corrections.

5 Possible use of $\delta O_2/N_2$ and $\delta^{18}O_{atm}$ for testing or improving the EDC3 glaciological age scale?

5.1 Testing EDC3 using $\delta O_2/N_2$ and local insolation

In the previous section we showed that both correlation analysis and time delay analysis display slightly different results depending on the insolation target. Moreover, they are not constant through time. These difference could have several origins/implications: (1) a systematic bias of the EDC3 age scale toward too old ages over the 300–800 ka period; (2) the target curve for $\delta O_2/N_2$ record over 300–800 ka at Dome C should be insolation at another date than the 21 December or integrated over another period than one centered around the 21 December.

If the problem is in the EDC3 age scale, the correlation and time delays between $\delta O_2/N_2$ and insolation variations enable an independent estimate of the EDC3 age scale uncertainty. Our data suggest that the EDC3 dating is correct within ±2.5 kyrs (i.e. 2 kyrs due to the average time delay depending on target insolation curve plus 0.5 kyr due to uncertainty in the filtering) over the period 300–800 ka, with the exception of four intervals marked by larger uncertainties. During the periods 390–460 ka, around 550 ka, around 650 ka (we note lower confidence over this period, as shown in Fig. 5) and around 750 ka, the EDC3 age scale uncertainty could be as high as ±5 kyrs (i.e., 4 kyrs due to the time delay including the uncertainty on the proper correct target curve plus up to 1 kyr due to uncertainty in the filtering method).

Our results have important implications for the uncertainties linked with the $\delta O_2/N_2$ orbital dating method. Our tests on the EDC $\delta O_2/N_2$ record suggest that the uncertainty associated with the orbital tuning parameter should take into account the effects of filtering and the choice of the target insolation series. These two uncertainties together are of the order of 2.5 kyrs (up to 5 kyrs) in our study. Our orbital dating using the current $\delta O_2/N_2$ record from the EDC ice core is clearly less precise than radiometric age markers derived from speleothems with an uncertainty of the order of 1 kyr (Cheng et al., 2009; Drysdale et al., 2009). Kawamura et al. (2007) take advantage of the similar variations of isotopic records of low latitudes speleothems and records of CH_4 trapped in polar ice cores to derive control points for ice core dating and to validate their $\delta O_2/N_2$ dating. Unfortunately, these age markers are so far limited to the last 400 ka (Cheng et al., 2009) and they cannot be used to test the uncertainty of the EDC3 timescale and the $\delta O_2/N_2$ constraints between 400 and 800 ka.

We now examine the opportunity to improve the EDC3 age scale by tuning our $\delta O_2/N_2$ record on the insolation curve on the 21 December as already done for the Vostok and Dome F ice cores. A systematic peak to peak correspondence as used in these previous studies is sometimes difficult to identify, in particular during periods with low eccentricity. A first example can be seen over the low eccentricity period between 390 and 460 ka, when the insolation curves display two small peaks or shoulders at 405 and 424 ka (Fig. 7). Neither of these secondary peaks is clearly identifiable in our filtered $\delta O_2/N_2$ signal nor in the original $\delta O_2/N_2$ record. This may arise because our $\delta O_2/N_2$ record is of too poor quality, with a variability so impacted by gas loss that the missing $\delta O_2/N_2$ variations lay within the noise; or because such small variations of insolation do not have significant impact on the processes controlling $\delta O_2/N_2$. Whatever the causes of such mismatch, the time difference between the two insolation minima on each side of the small peaks reaches up to 20 kyrs (for the 405 ka peak). This difference will lead to a tuning uncertainty of up to ±10 kyrs over this period, if we match the peaks of the $\delta O_2/N_2$ record with the mid-peaks of the insolation target curve as is classically done. A second example is the minimum of insolation at 750 ka: here

CPD
7, 2217–2259, 2011

the number of peaks is similar between the $\delta O_2/N_2$ and the insolation curves. Still, an unambiguous identification is difficult, as shown by a time delay of 4–5 kyrs. In turn, caution should be taken, at least for the EDC record, when tuning $\delta O_2/N_2$ variations to the summer insolation curve over periods of low eccentricity for which high precision (i.e. ice stored at −50°C) and high resolution $\delta O_2/N_2$ data are in any case needed.

5.2 Combined use of $\delta O_2/N_2$ and $\delta^{18}O_{atm}$

The isotopic composition of oxygen in the atmosphere ($\delta^{18}O_{atm}$) can be recovered from the isotopic analysis of $\delta^{18}O$ in air trapped in ice cores, after correction for gravitational fractionation. This parameter has been used in many previous dating studies because of its strong link to precession (Petit et al., 1999; Shackleton et al., 2000; Dreyfus et al., 2007). Figure 7 displays the relationship between the $\delta^{18}O_{atm}$ record from the EDC ice core (Dreyfus et al., 2007) and the precession parameter over the period 306–796 ka (1 kyr re-sampling and 15–100 kyrs band pass filter). Dreyfus et al. (2007) and Landais et al. (2010) have already shown the high correlation between $\delta^{18}O_{atm}$ and precession over this time period. Here, we additionally display the time delay between $\delta^{18}O_{atm}$ and precession (Fig. 7). On average, this time delay is around 5.5 kyrs, i.e. very similar to what is observed over the last deglaciation (Dreyfus et al., 2007). Over the last deglaciation, this time delay is mainly due to the interplay between a strong ice sheet melting and weak monsoon intervals (Cheng et al., 2009). Because of the complex interplay of ice sheet melting, biosphere and hydrological cycle influences on $\delta^{18}O_{atm}$ that strongly varies from one period to another (strong melting of ice sheets occurs only during deglaciations), we do not expect a priori that this time delay remains constant with time. However, what we observe in Fig. 7 is that this time delay remains constant within ±1 kyr except between 360 and 450 ka and around 750 ka (and, to a weaker extent, around 550 ka and 650 ka), i.e. over the periods where the comparison of $\delta O_2/N_2$ and insolation curves has revealed that the EDC3 age scale was correct within the published uncertainty. This analysis suggests that the phase lag of $\delta^{18}O_{atm}$ is relatively

CPD
7, 2217–2259, 2011

cc BY

constant, however, the 6 kyrs precision of the EDC chronology does not allow us to exclude variations in phase at the 1-kyr scale. There can be two alternative explanations for the strongest changing phase lags between precession and $\delta^{18}O_{atm}$ and between summer insolation and $\delta O_2/N_2$ between 360 and 450 ka and around 750 ka. It is possible that changes in local summer insolation and precession (due to low eccentricity) are too small to affect EDC $\delta O_2/N_2$ and $\delta^{18}O_{atm}$, both being then controlled by other parameters (i.e. mean annual temperature, accumulation rate or natural atmospheric variations for $\delta O_2/N_2$, ice volume and hydrology for $\delta^{18}O_{atm}$). Alternatively, the mismatch could be due to the EDC3 chronology which should then be corrected for these two time periods.

5.3 Example of dating constraints and limitations: MIS 11 duration from the $\delta O_2/N_2$ record

Marine Isotopic Stage 11 is 31.7 kyrs long on the EDC3 age scale (Parrenin et al., 2007) using a threshold of −403 ‰ as the minimum δD value for the interglacial period (EPICA comm. members, 2004). MIS11 is the longest Antarctic warm period (or interglacial period as identified in Antarctic temperature proxies) over the last 800 ka (Jouzel et al, 2007). Such long duration of this interglacial period has been challenged by Lisiecki and Raymo (2005) and Kawamura et al. (2009). Following our suggestion that EDC3 should perhaps be reexamined between 390 and 450 ka, we apply the orbital $\delta O_2/N_2$ tuning method on the EDC ice core MIS11 interval to propose a minimal and maximal duration for this interglacial period.

With this aim, we present in Fig. 8 a comparison of filtered 21 December insolation and $\delta O_2/N_2$ and two possible peak-to-peak correspondences between the two curves (green and blue arrows). As already mentioned, this peak matching is ambiguous because orbital peaks may be missing in the $\delta O_2/N_2$ record in this period of low eccentricity. This ambiguity leads us to propose two possible scenarios compatible with this orbital tuning, as depicted in Fig. 8, with one representing the minimum duration of 20.4 kyrs (green curve) and the other representing a maximum duration of 34.7 kyrs

CPD
7, 2217–2259, 2011
Towards orbital dating of the EPICA Dome C ice core
A. Landais et al.

Discussion Paper | Discussion Paper | Discussion Paper | Discussion Paper |

(blue curve), compared with the duration of 31.7 kyrs in the EDC3 age scale. Even the minimum duration for MIS 11 of 20.4 kyrs confirms that it is an unusually long warm phase.

MIS 11 is a problematic period to date with $\delta O_2/N_2$ because of low eccentricity as amply discussed above. Additional uncertainties over this time period are caused by (1) the combination of $\delta O_2/N_2$ performed on ice kept at −25 °C (after 380 ka) and kept at −50 °C (before 380 ka) and (2) a discrepancy between the filtered and the original $\delta O_2/N_2$ records around 360 ka. Analysis of $\delta O_2/N_2$ on fresh ice over the period covering 350 to 380 ka is thus needed before we can offer a proper new dating of MIS 11 in the EDC ice core. Nevertheless, the range of MIS11 durations proposed here has been used to study the impact of dating uncertainties on the suborbital climate variability within this warm interval (Pol et al., 2010).

6 Conclusion and perspectives

We have presented the first record of $\delta O_2/N_2$ over the EDC ice core covering the period between 306 and 796 ka. Most of the samples were stored at −25 °C for 1 yr or more before their analysis so that raw $\delta O_2/N_2$ measurements are strongly affected by gas loss fractionation. Using high precision $\delta O_2/N_2$ measurements performed on similar depths on EDC samples carefully kept frozen at −50 °C, we were able to propose two gas loss corrections to build composite $\delta O_2/N_2$ curves. Using one or another gas loss correction has no significant influence on the orbital chronology issue. However, the band pass filtering method on our $\delta O_2/N_2$ record can lead to an uncertainty of the order of 1 kyr.

The frequency spectrum of EDC $\delta O_2/N_2$ composite curves and of local insolation of 21 December 75° S are very similar over the period 300–800 ka as previously observed for other ice core $\delta O_2/N_2$ records over the 0–400 ka period. Following previous studies performed on the Vostok and Dome F ice cores over the last 400 ka, we have explored the added value of the $\delta O_2/N_2$ signal to test the EDC3 age scale over the

CC BY

period 300–800 ka. In our case, the time correspondence of $\delta O_2/N_2$ with 21 December insolation is not obvious because (1) the correlation of $\delta O_2/N_2$ is sometimes better with the 21 December −21 March local insolation curve than with the 21 December local insolation curve (relative phase shift of 2 kyrs between these insolation targets) and (2) there is a mean time delay of 2 kyrs between our filtered $\delta O_2/N_2$ record and the 21 December local insolation. Moreover, we have shown that for low eccentricity time periods, it remains a challenge to identify unambiguously peak-to-peak correspondence between $\delta O_2/N_2$ and insolation. These two effects result in a large uncertainty (more than 10 kyrs locally) in the determination of a new chronology, which prevents us from using the current $\delta O_2/N_2$ record to produce a new EDC age scale.

Even if we call for cautiousness in the use of $\delta O_2/N_2$ as an unambiguous dating tool and if this uncertainty prevents us from using our $\delta O_2/N_2$ constraints for building a new EDC age scale, we can still use the comparison between $\delta O_2/N_2$ and the local 21 December insolation to test the current EDC3 chronology. First, we show that over the major part of the 300–800 ka period, EDC3 is correct within the published uncertainty (6 kyrs). We however identify several specific periods where the shift between $\delta O_2/N_2$ record and the local 21 December insolation signal shows strong variations. The identification of problematic time intervals in the EDC3 age scale is strengthened by consistent anomalies observed in the time delays of $\delta O_2/N_2$ vs. local summer insolation and of $\delta^{18}O_{atm}$ vs. precession. These anomalies are observed during periods of low eccentricity and suggest either that $\delta O_2/N_2$ and $\delta^{18}O_{atm}$ can not be used as dating constraints during minima of eccentricity, or that the EDC3 age scale should be revised over the following periods: 360–450 ka and 720–760 ka (possibly 520–560 ka). For the exceptional but uncertainty length of MIS 11 interglacial, our $\delta O_2/N_2$ constraint allows us to propose a minimum duration of 20.4 ka and a maximum duration of 34.7 ka.

In order to improve the dating of the oldest Antarctic records (EDC and Dome F), it would be valuable to produce high accuracy records of total air content, $\delta O_2/N_2$ and $\delta^{18}O_{atm}$ over the period 300–800 ka with a focus on the period 350 to 390 ka to improve our constraint on the length of MIS 11. The consistency of the various records

Discussion Paper | Discussion Paper | Discussion Paper | Discussion Paper |
CPD
7, 2217–2259, 2011

in two ice cores would allow us to establish improved age scales. Our long $\delta O_2/N_2$ record further reveals that the variance of the signal is preserved back to 800 ka even close to bedrock, and that, if stored at −50 °C, deep and old ice can provide accurate $\delta O_2/N_2$ records. This has strong implications for the IPICS (International Partnerships in Ice Core Sciences) oldest ice challenge, with the target to obtain Antarctic ice cores spanning more than one million years and to date them.

Acknowledgements. We would like to thank Bénédicte Minster for the help in the measurements as well as Catherine Ritz, Olivier Cattani and Sonia Falourd for the complex logistics involved in cutting and transporting EDC samples at −50 °C from Dome C to our laboratory. We thank Frédéric Parrenin as well as 3 reviewers for constructive comments allowing very significant improvements of this manuscript. Kenji Kawamura is deeply acknowledged for having provided the results of the filtering method described in Kawamura et al. (2007) applied on our set of data. This project was funded by the European project EPICA-MIS and the French ANR PICC project. G. Dreyfus acknowledges support from the National Science Foundation Graduate Research Fellowship program and the Commissariat à l'Energie Atomique. This work is a contribution to the European Project for Ice Coring in Antarctica (EPICA), a joint European Science Foundation/European Commission scientific programme, funded by the EU (EPICA-MIS) and by national contributions from Belgium, Denmark, France, Germany, Italy, the Netherlands, Norway, Sweden, Switzerland and the United Kingdom. The main logistic was provided by IPEV and PNRA (at Dome C) and AWI (at Dronning Maud Land). This is a contribution to the European project PAST4FUTURE.

The publication of this article is financed by CNRS-INSU.

References

Aciego, S., Bourdon, B., Schwander, J., Baur, H., and Forieri, A.: Toward a radiometric ice clock: U-series of the Dome C ice core, TALDICE-EPICA science meeting, April 12–15, Rome (Italy), 2010.

Bar-Matthews, M., Ayalon, A., Gilmour, M., Matthews, A., and Hawkesworth, C. J.: Sea-land oxygen isotopic relationships from planktonic foraminifera and speleothems in the Eastern Mediterranean region and their implication for paleorainfall during interglacial intervals, Geochim. Cosmochim. Acta, 67, 3181–3199, 2003.

Battle, M., Bender, M. L., Sowers, T., Tans, P. P., Butler, J. H., Elkins, J. W., Ellis, J. T., Conway, T., Zhang, N., Lang, P., and Clarke, A. D.: Atmospheric gas concentrations over the past century measured in air from firn at the South Pole, Nature, 383, 231–235, 1996.

Bender, M. L.: Orbital tuning chronology for the Vostok climate record supported by trapped gas composition, Earth Planet. Sci. Lett., 204, 275–289, 2002.

Bender, M., Sowers, T., and Labeyrie, L.: The Dole effect and its variations during the last 130,000 years as measured in the Vostok ice core, Global Biogeochem. Cy., 8, 363–376, 1994.

Bender, M., Sowers, T., and Lipenkov, V.: On the concentrations of O_2, N_2 and Ar in trapped gases from ice cores: J. Geophys. Res., 100, 18651–18660, 1995.

Berger A. and Loutre, M. F.: Insolation values for the climate of the last 10 million years, Quat. Sci. Rev., 10, 297–317, 1991.

Berger A. and Loutre, M. F.: Long-term variations of the astronomical seasons. In: Topics in Atmospheric and Interstellar Physics and Chemistry. Cl. Boutron (ed), Les Editions de Physique, Les Ulis, France, 33–61, 1994.

Berger A. and Loutre, M. F.: Astronomical theory of climatic change, in: From Indoor Air Pollution to the Search for the Earth like Planets in the Cosmos, edited by: Boutron, C., Journal de Physique IV, vol. 121, EDP, Sciences, Les Ulis, 2004, 1–35.

Blunier T., Spahni, R., Barnola, J.-M., Chappellaz, J., Loulergue, L., and Schwander, J.: Synchronization of ice core records via atmospheric gases, Clim. Past, 3, 325–330, 2007.

Chappellaz, J., Blunier, T., Raynaud, D., Barnola, J.-M., Schwander, J., and Stauffer, B.: Synchronous Changes in Atmospheric CH_4 and Greenland Climate between 40 kyr and 8 kyr BP, Nature, 366, 6454, 443–445, 1993.

Dreyfus, G. B.: La composition isotopique de l'air piégé dans la glace: interprétation climatique

CPD
7, 2217–2259, 2011

Towards orbital dating of the EPICA Dome C ice core

A. Landais et al.

CC BY

et outil chronologique. Thèse de doctorat de l'Université Pierre et Marie Curie, Paris 6, 1–173, 2008.
Dreyfus, G. B., Parrenin, F., Lemieux-Dudon, B., Durand, G., Masson-Delmotte, V., Jouzel, J., Barnola, J.-M., Panno, L., Spahni, R., Tisserand, A., Siegenthaler, U., and Leuenberger, M.: Anomalous flow below 2700 m in the EPICA Dome C ice core detected using $\delta^{18}O$ of atmospheric oxygen measurements, Clim. Past, 3, 341–353, doi:10.5194/cp-3-341-2007, 2007.
Dunbar, N., McIntosh, W., and Esser, R.: Physical setting and tephrochronology of the summit Caldera ice record at Mount Moulton, West Antarctica, Bull. Geol. Soc. Am., 7–8, 796–812, 2008.
Durand, G., Svensson, A., Persson, A., Gagliardini, O., Gillet-Chaulet, F., Sjolte, J., Montagnat, M., Dahl-Jensen, D.: Evolution of the texture along the EPICA Dome C ice core, Physics of ice core records II, T. Hondoh, Hokkaido University press, 91–106, 2010.
EPICA comm. members: Eight glacial cycles from an Antarctic ice core, Nature, 429, 623–628, 2004.
Hoffmann, G., Cuntz, M., Weber, C., Ciais, P., Friedlingstein, P., Heimann, M., Jouzel, J., Kaduk, J. Maier-Reimer, E., Seibt, U., and Six, K.: A model of the Earth's Dole effect, Global Biogeochem. Cy., 18(1), GB1008, doi:10.1029/2003GB002059, 2004.
Huber, C., Beyerle, U., Leuenberger, M., Schwander, J., Kipfer, R., Spahni, R., Severinghaus, J. P., and Weiler, K.: Evidence for molecular size dependent gas fractionation in firn air derived from noble gases, oxygen and nitrogen measurements, Earth Planet Sci. Lett., 243, 61–73, 2006.
Hutterli, M. A., Schneebeli, M., Freitag, J., Kipfstuhl, J., and Rothlisberger, R.: Impact of local insolation on snow metamorphism and ice core records, Physics of ice core records II, T. Hondoh, Hokkaido University press, 223–232, 2010.
Huybers, P. and Denton, G.: Antarctic temperature at orbital time scales controlled by local summer duration, Nat. Geosci., 1, 787–792, 2008.
Ikeda-Fukazawa, T., Fukumizu, K., Kawamura, K., Aoki, S., Nakazawa, T., and Hondoh, T.: Effects of molecular diffusion on trapped gas composition in polar ice cores, Earth Planet Sci. Lett., 229, 183–192, 2005.
Jouzel, J., Hoffmann, G., Parrenin, F., and Waelbroeck, C.: Atmospheric oxygen 18 and sea-level changes, Quat. Sci. Rev., 21, 1–3, 2002.
Jouzel, J., Masson-Delmotte, V., Cattani, O., Dreyfus, G., Falourd, S., Hoffmann, G., Minster, B.,

CPD
7, 2217–2259, 2011

Towards orbital dating of the EPICA Dome C ice core

A. Landais et al.

CC BY

Nouet, J., Barnola, J.-M., Fisher, H., Gallet, J.-C., Johnsen, S., Leuenberger, M., Loulergue, L., Luethi, D., Oerter, H., Parrenin, F., Raisbeck, G., Raynaud, D., Schilt, A., Schwander, J., Selmo, J., Souchez, R., Spahni, R., Stauffer, B., Steffensen, J.P., Stenni, B., Stocker, T.F., Tison, J.-L., Werner, M., and Wolff, E.W.: Orbital and millennial Antarctic climate variability over the past 800,000 years, Science, 317, 793–796, 2007.

Kawamura, K., Nakazawa, T., Aoki, S., Sugawara, S., Fuji, Y., and Wanatabe, O.: Atmospheric CO_2 variations over the last three glacial-interglacial climatic cycles deduced from the Dome Fuji deep ice core, Antarctica using a wet extraction technique, Tellus, 55B, 126–137, 2003.

Kawamura, K., Parrenin, F., Lisiecki, L., Uemura, R., Vimeux, F., Severinghaus, J. P., Hutterli, M. A., Nakazawa, T., Aoki, S., Jouzel, J., Raymo, M. E., Matsumoto, K., Nakata, H., Motoyama, H., Fujita, S., Goto-Azuma, K., Fujii, K., and Watanabe, O.: Northern hemisphere forcing of climatic cyles over the past 360,000 years implied by accurately dated Antarctic ice cores, Nature, 448, 912–916, 2007.

Kawamura, K., Aoki, S., and Nakazawa, T.: Accurate chronology of the Dome Fuji ice core based on O_2/N_2 ratio of trapped air, PAGES OSM, Corvallis, July 2009.

Landais, A., Caillon, N., Severinghaus, J., Jouzel, J., and Masson-Delmotte, V.: Analyses isotopiques à haute précision de l'air piégé dans les glaces polaires pour la quantification des variations rapides de température: méthodes et limites, Notes des activités instrumentales de l'IPSL, 39, 2003.

Landais, A., Dreyfus, D., Capron, E., Sanchez-Goni, M. F., Desprat, S., Jouzel, J., Hoffmann, G., and Johnsen, S.: What drive orbital- and millennial-scale variations of the $\delta^{18}O$ of atmospheric oxygen?, Quat.Sci.Rev, 29, 235–246, 2010.

Lemieux-Dudon, B., Blayo, E., Petit, J.-R., Waelbroeck, C., Svensson, A., Ritz, C., Barnola, J.-M., Narcisi, B.-M., and Parrenin, F.: Consistent dating for Greenland and Antarctic ice cores, Quat. Sci. Rev, 29, 8–20, 2010.

Leuenberger, M.: Modeling the signal transfer of seawater $\delta^{18}O$ to the $\delta^{18}O$ of atmospheric oxygen using a diagnostic box model for the terrestrial and marine biosphere, J. Geophys. Res., 102(C12), 26841–26850, 1997.

Lisiecki, L. E. and Raymo, M. E.: A Pliocene-Pleistocene stack of 57 globally distributed benthic $\delta^{18}O$ records, Paleoceanography, 20, PA1003, doi:10.1029/2004PA001071, 2005.

Loulergue, L., Schilt, A., Spahni, R., Masson-Delmotte, V., Blunier, T., Lemieux, B., Barnola, J.-M., Raynaud, D., Stocker, T. F., and Chappellaz, J.: Orbital and millennial-scale features of atmospheric CH_4 over the past 800,000 years, Nature, 453(7193), 383–386, 2008.

Loutre, M. F. and Berger, A.: Stage 11 as an analogue for the present interglacial., Global Planet. Change, doi:10.1016/S0921-8181(02)00186-8, 36(3), 209–217, 2003.

Loutre, M. F., Paillard, D., Vimeux, F., and Cortijo, E.: Does mean annual insolation hace the potential to change the climate?, Earth Planet Sci. Lett., 221(1–4), 1–14, 2004.

Lüthi, D., Le Floch, M., Bereiter, B., Blunier, T., Barnola, J.-M., Siegenthaler, U., Raynaud, D., Jouzel, J., Fischer, H., Kawamura, K., and Stocker, T. F.: High-resolution carbon dioxide concentration record 650,000–800,000 years before present, Nature, 453, 379–382, 2008.

Mallat, S.: A wavelet Tour of Signal Processing, Academic Press, San Diego, CA, USA, 577, 1998.

Martinson, D. G., Pisias, N. G., Hays, J. D., Imbrie, J., Moore, T. C., and Shackleton, N. J.: Age dating and the orbital theory of the ice ages: Development of a high resolution 0 to 300 000 year chronostratigraphy, Quaternary Research, 27(1), 1–29, 1987.

Melice, J. L. and Servain, J.: The tropical Atlantic meridional SST gradient index and its relationships with the SOI, NAO and Southern Ocean, Clim. Dyn., 20, 447–464, doi:10.1007/s00382-002-0289, 2003.

Milankovitch, M.: Kanon der Erdbestrahlung und seine Anwendung auf das Eiszeitenproblem, Royal Serbian Sciences, Spec. pub. 132, section of Mathematical and Natural Sciences, 33, Belgrade, 633, 1941.

Paillard, D., Labeyrie, L., and Yiou, P.: Macintosh program performs time-series Analysis. Eos Trans. AGU, 77(39), 379, 1996.

Parrenin, F., Barnola, J.-M., Beer, J., Blunier, T., Castellano, E., Chappellaz, J., Dreyfus, G., Fischer, H., Fujita, S., Jouzel, J., Kawamura, K., Lemieux-Dudon, B., Loulergue, L., Masson-Delmotte, V., Narcisi, B., Petit, J.-R., Raisbeck, G., Raynaud, D., Ruth, U., Schwander, J., Severi, M., Spahni, R., Steffensen, J. P., Svensson, A., Udisti, R., Waelbroeck, C., and Wolff, E.: The EDC3 chronology for the EPICA Dome C ice core, Clim. Past, 3, 485–497, doi:10.5194/cp-3-485-2007, 2007.

Petit, J. R., Jouzel, J., Raynaud, D., Barkov, N. I., Barnola, J. M., Basile, I., Bender, M., Chappellaz, J., Davis, M., Delaygue, G., Delmotte, M., Kotlyakov, V. M., Legrand, M., Lipenkov, V., Lorius, C., Pepin, L., Ritz, C., Saltzman, E., and Stievenard, M.: Climate and atmospheric history of the past 420 000 years from the Vostok ice core, Nature, 399,429–436, 1999.

Pol, K., Masson-Delmotte, V., Johnsen, S., Bigler, M., Cattani, O., Durand, G., Falourd, S., Jouzel, J., Minster, B., Parrenin, F., Ritz, C., Steen-Larsen, H. C., and Stenni, B.: New MIS 19 EPICA Dome C high resolution deuterium data: hints for a problematic preser-

vation of climate variability in the "oldest ice", Earth Planet. Sci. Lett., 298(1–2), 95–103, doi:10.1016/j.epsl.2010.07.030, 2010.
Pol, K., Debret, M., Masson-Delmotte, V., Capron, E., Cattani, O., Dreyfus, G., Falourd, S., Johnsen, S., Jouzel, J., Landais, A., Minster, B., and Stenni, B.: Links between MIS 11 millennial to sub-millennial climate variability and long term trends as revealed by new high resolution EPICA Dome C deuterium data A comparison with the Holocene, Clim. Past, 7, 437–450, doi:10.5194/cp-7-437-2011, 2011.
Raisbeck, G. M., Yiou, F., Jouzel, J., and Stocker, T. F.: Direct north-south synchronization of abrupt climate change record in ice cores using Beryllium 10, Clim. Past, 3, 541–547, doi:10.5194/cp-3-541-2007, 2007.
Rasmussen, S. O., Andersen, K. K., Svensson, A. M., Steffensen, J. P., Vinther, B. M., Clausen, H. B., Andersen, M.-L. S., Johnsen, S. J., Larsen, L. B., Bigler, M., Rothlisberger, R., Fischer, H., Goto-Azuma, K., Hansson, M. E., and Ruth, U.: A new Greenland ice core chronology for the last glacial termination, J. Geophys. Res., 111, D06102, doi:10.1029/2005JD006079, 2006.
Raynaud, D., Lipenkov, V., Lemieux-Dudon, B., Duval, P., Loutre, M.-F., and Lhomme, N.: The local insolation signature of air content in Antarctic ice. A new step toward an absolute dating of ice records, Earth Planet. Sci. Lett., 261, 337–349, 2007.
Ruddiman, W. F. and Raymo, M. E.: A methane-based time scale for Vostok ice, Quat. Sci. Rev, 22, 141–155, 2003.
Schmidt, G. A., Shindell, D. T., and Harder, S.: A note on the relationship between ice core methane concentrations and insolation, Geophys. Res. Lett., 31, L23206, doi:10.1029/2004GL021083, 2004.
Severinghaus, J. P. and Battle, M. O.: Fractionation of gases in polar ice during bubble close-off: New constraints from firn air Ne, Kr and Xe observations, Earth Planet Sci. Lett., 244(1–2), 474-500, 2006.
Shackleton, N. J., Hall, M. A., and Vincent, E.: Phase relationships between millennial-scale events 64,000–24,000 years ago: Paleoceanography, 15, 565–569, 2000.
Sowers, T., Bender, M., and Raynaud, D.: Elemental and isotopic composition of occluded O_2 and N_2 in polar ice, J. Geophys. Res., 94(D4), 5137–515, 1989.
Suwa, M. and Bender, M. L.: O_2/N_2 ratios of occluded air in the GISP2 ice core, J. Geophys. Res., 113(D11), D11119, doi:11110.11029/12007JD009589, 2008a.
Suwa, M. and Bender, M. L.: Chronology of the Vostok ice core constrained by O_2/N_2 ratios of

cc BY

occluded air, and its implication for the Vostok climate records, Quat. Sci. Rev., 27, 1093–1106, 2008b.

Svensson, A., Andersen, K. K., Bigler, M., Clausen, H. B., Dahl-Jensen, D., Davies, S. M., Johnsen, S. J., Muscheler, R., Rasmussen, S. O., Röthlisberger, R., Steffensen, J. P., and Vinther, B. M.: The Greenland Ice Core Chronology 2005, 15–41 kyr. Part 2: Comparison to other records, Quat.Sci.Rev, 25, 3258–3267, 2006.

Svensson, A., Andersen, K. K., Bigler, M., Clausen, H. B., Dahl-Jensen, D., Davies, S. M., Johnsen, S. J., Muscheler, R., Parrenin, F., Rasmussen, S. O., Rthlisberger, R., Seierstad, I., Steffensen, J. P., and Vinther, B. M.: A 60 000 year Greenland stratigraphic ice core chronology, Clim. Past, 4, 47–57, doi:10.5194/cp-4-47-2008, 2008.

Torrence, C. and Compo, G. P.: A practical guide to wavelet analysis, Bull. Am. Meteorol. Soc., 79, 61–78, 1999.

Yiou, F., Raisbeck, G. M., Baumgartner, S., Beer, J., Hammer, C., Johnsen, S., Jouzel, J., Kubik, P. W., Lestringuez, J., Stievenard, M., Suter, M., and Yiou, P.: Beryllium 10 in the Greenland Ice Core Project ice core at Summit, Greenland, J. Geophys. Res., 102(C12), 26783–26794, 1997.

CC BY

Table 1. Details of the 4 different series of $\delta O_2/N_2$ data measured at LSCE on the EDC ice core (see also Fig. 1). We indicate the number of the series as referenced in the text, the number of depth levels studied, the mean depth interval, the mass spectrometer on which the $\delta O_2/N_2$ measurements were carried, the year when the analyses were performed, the pooled standard deviation and the numbers of depth levels rejected associated with each series. Series 1 and 2 were obtained from ice stored at −25 °C while series 3 and 4 were obtained from ice stored at −50 °C.

Series	Depth levels	Depth resolution	Mass Spectrometer	Year (A.D.)	Pooled standard deviation (‰)	Number of outliers
1 (red)	109	3 to 4 m between 2483–2850 m 20 m between 2850–3100 m	Finnigan MAT 252	2005	1.2	10
2 (green)	112	20 m between 2800–3040 m 1.5 m between 3040–3200 m	Thermo Delta V Plus	2006	1.96	23 (14 below 3100 m depth)
3 (blue)	30	2.5 m between 2822–2893 m	Thermo Delta V Plus	2007	0.32	0
4 (purple)	29	2.5 m between 3105 and 3188 m	Thermo Delta V Plus	2008	1.03	0

Discussion Paper | Discussion Paper | Discussion Paper | Discussion Paper |

CPD

7, 2217–2259, 2011

Towards orbital dating of the EPICA Dome C ice core

A. Landais et al.

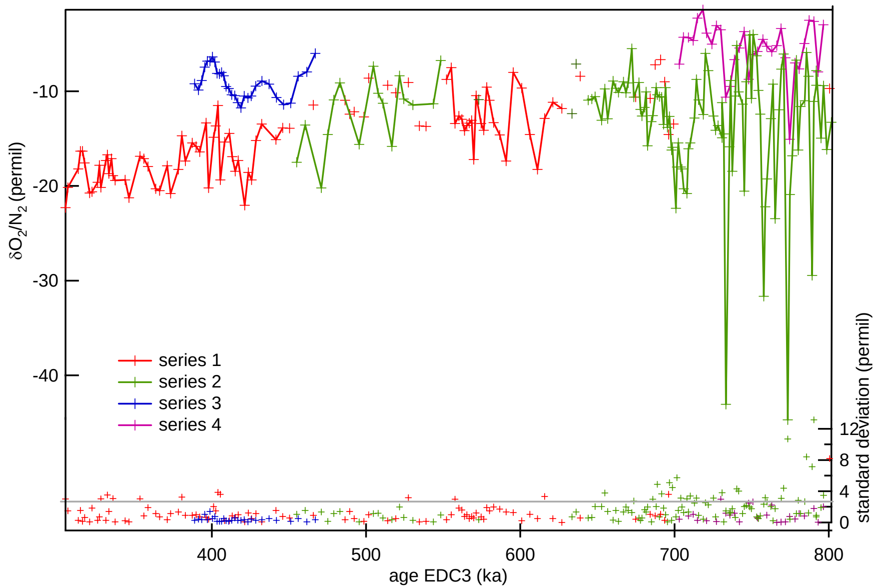

Fig. 1. Measurements of $\delta O_2/N_2$ in the EPICA Dome C (EDC) ice core plotted on the EDC3 ice core age scale (Parrenin et al, 2007) and associated uncertainty (1σ, bottom). The EDC $\delta O_2/N_2$ record is composed of four distinct measurement series (top). Samples measured in series 1 and 2 were stored at −25 °C whereas samples measured in series 3 and 4 were stored at −50 °C. Characteristics of the different series are given in Table 1: series 1 in red, series 2 in green, series 3 in blue, series 4 in purple.

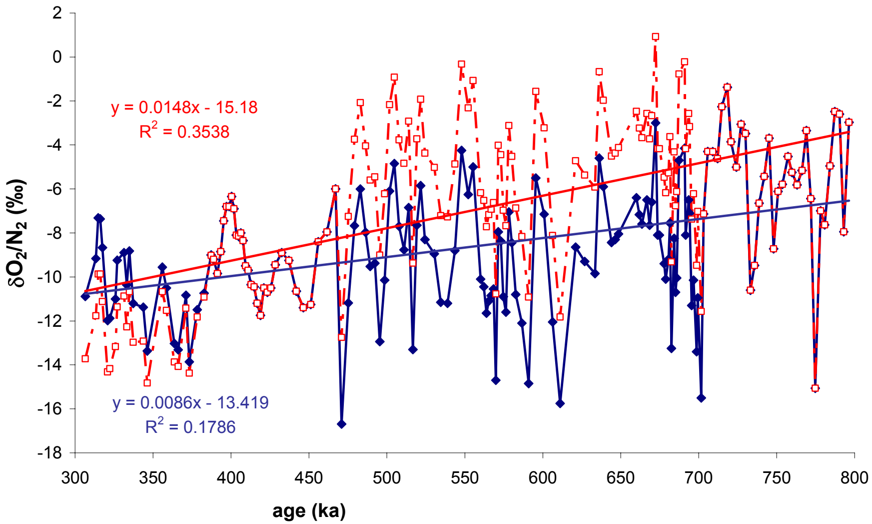

Fig. 2. Two gas loss corrections for the EDC $\delta O_2/N_2$ record. Gas loss during storage occurs more quickly for O_2 than N_2 and the rate of loss increases with temperature (Ikeda-Fukazawa et al., 2005). Without any accurate storage temperature history documentation, we propose two gas loss corrections: "gas correction 1" (curve 1 = red) shifts all Series 1 and 2 data by +6.43 ‰ (the average offset between Series 1 and 2 when compared with Series 3), resulting in a variance of 13 ‰ after outlier rejection; "gas correction 2" (curve 2 = blue) seeks to homogenize Series 1 and 2 with Series 3 and 4 where they overlap.

CC BY

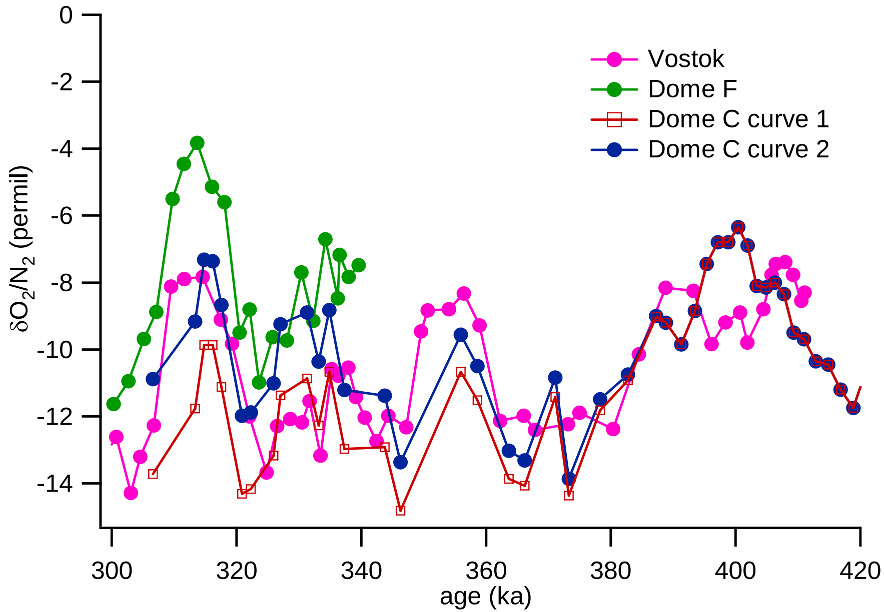

Fig. 3. Comparison between the two composite EDC $\delta O_2/N_2$ curves and existing $\delta O_2/N_2$ records from Dome F (Kawamura et al., 2007) and Vostok (Bender et al., 2002; Suwa and Bender, 2008). Because of the different time periods covered by the different ice cores, the comparison is limited to the period 300–340 ka for Dome F and EDC and 300–410 ka for Vostok and EDC.

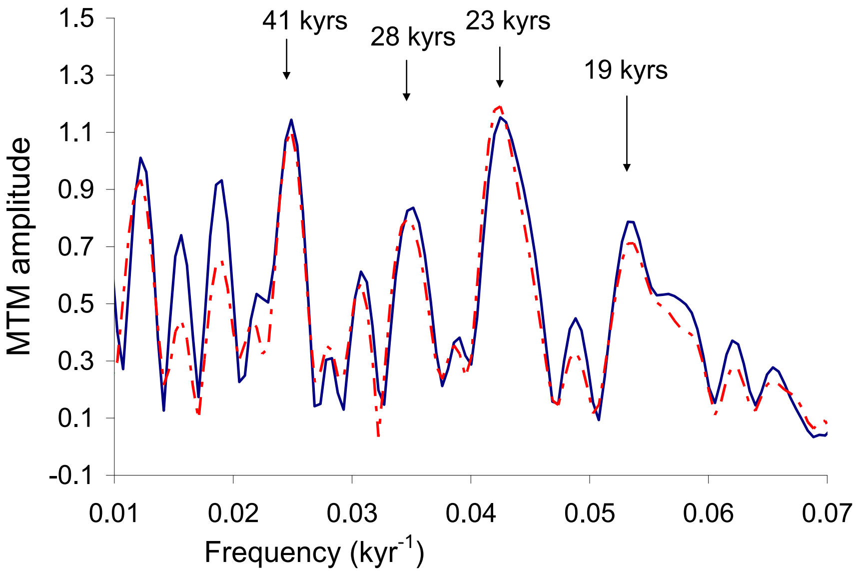

Fig. 4a. Spectral analysis (multi tapered method) of the $\delta O_2/N_2$ composite curves (gas loss correction 1 in red and gas loss correction 2 in blue). The significant peaks (>90 %) are identified with an arrow on top.

CC BY

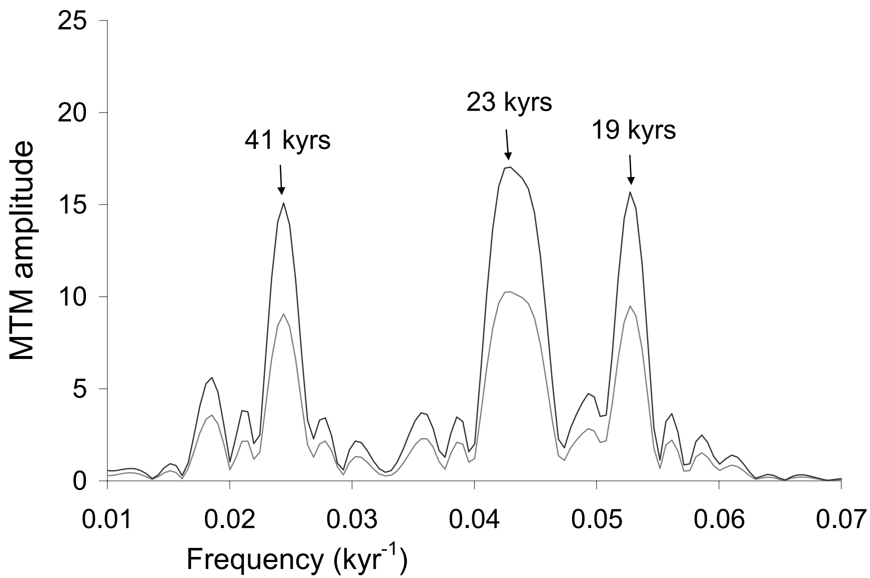

Fig. 4b. Spectral analysis (multi tapered method) of the insolation curves (black: 21 December insolation at 75° S; grey: 21 December–21 March insolation at 75° S). The significant peaks (>90 %) are identified with an arrow on top.

CPD
7, 2217–2259, 2011

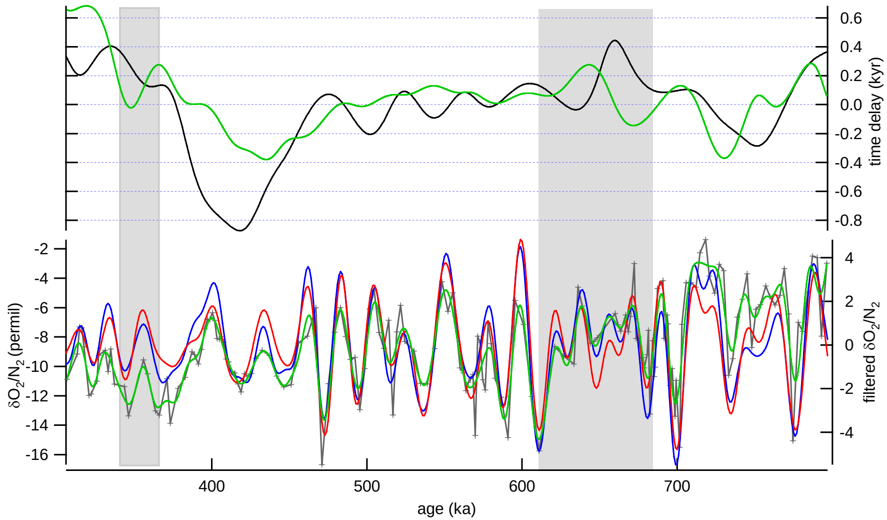

Fig. 5. Effect of band pass filtering of the $\delta O_2/N_2$ record. Bottom: Composite $\delta O_2/N_2$ data (curve 2, dark grey). Resampled (1 kyr) and filtered $\delta O_2/N_2$ signal with "gas loss correction 2" (i.e. curve 2) for frequencies corresponding to 15–100 kyrs (blue) and 15–60 kyrs (red). The effect of the Kaiser window filter described in Kawamura et al. (2007) is displayed in green. Top: time delay between the filtered curves at 15–100 kyrs and at 15–60 kyrs (black). The green curve indicates the time delay between the filtered curve at 15–100 kyrs and the one using the Kaiser window filter of Kawamura et al. (2007). The grey rectangles indicate the periods when the resolution of the $\delta O_2/N_2$ signal is too low (>3 kyrs), limiting the validity of the filtering.

CPD
7, 2217–2259, 2011

Towards orbital dating of the EPICA Dome C ice core

A. Landais et al.

CC BY

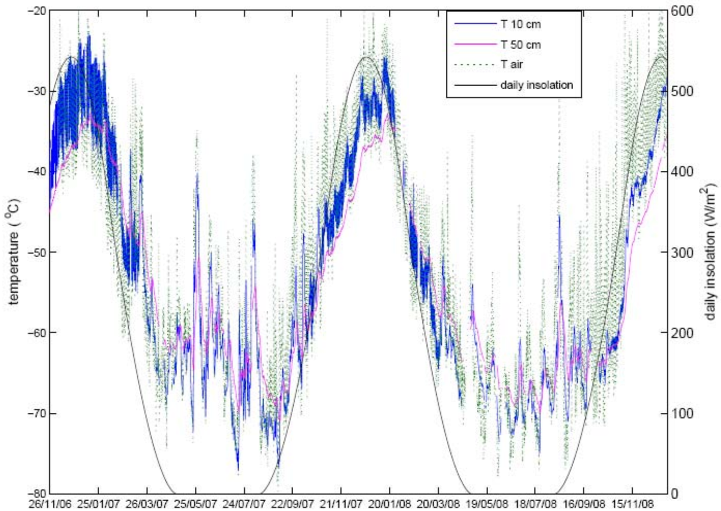

Fig. 6. Evolution of the daily insolation (black), air temperature (dotted green), snow temperature at 10 cm depth (blue) and temperature at 50 cm depth (pink) at the Dome C station between the year 2006 and 2008. The temperature measurements of the snow at Dome Concordia are part of a more complete system which records temperatures every hour at 40 levels from the surface down to 21 m since November 2006. Temperatures were measured with 100 ohm Platinum Resistance Temperature (PRT) detectors (IEC751 1/10 DIN). A more detailed description of the system and an open data access will be soon available on the OSUG website (http://www.obs.ujf-grenoble.fr).The air temperature sensor is housed in a naturally aspirated multi-plate radiation shield (Young 41003), and the measurement was performed at 1 m height. The lag between the maximum of snow temperatures measured at 10 cm and 50 cm is due to the diffusion time of the annual wave temperature between these two levels. The obvious decrease of the diurnal amplitude variations of T_10 cm during the observed period is due to the snow accumulation at the surface. This accumulation implies also an increase of the lag between air and snow temperature measurements.

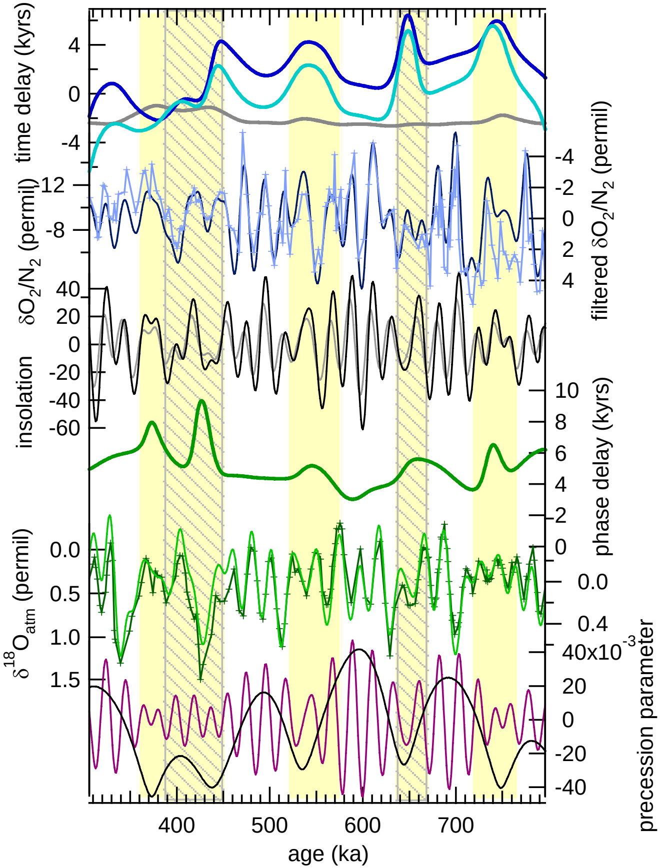

Fig. 7. Caption on next page.

Discussion Paper | Discussion Paper | Discussion Paper | Discussion Paper |

Fig. 7. Possible orbital constraints derived from $\delta O_2/N_2$ and $\delta^{18}O_{atm}$ records when compared respectively to the local 21 December insolation and precession curves. From top to bottom:

- Time delay between $\delta O_2/N_2$ (curve 2) and local summer insolation curves (dark blue: between $\delta O_2/N_2$ and 21 December insolation at 75° S; light blue: between $\delta O_2/N_2$ and 21 December and 21 March insolation at 75° S) and time delay between 21 December insolation and 21 December to 21 March insolation at 75° S (grey). The original series were first filtered before the computation of the time delay.
- $\delta O_2/N_2$ curve (curve 2) from the EDC ice core (light blue: raw data; dark blue: after 1 kyr re-sampling and band pass filtering between 15 and 100 kyrs). The corresponding Y-axis is reversed.
- 75°S summer insolation (black: 21 December; grey: 21 December to 21 March)
- Time delay between $\delta^{18}O_{atm}$ and precession. The original series were filtered before the computation of the time delay.
- $\delta^{18}O_{atm}$ record at EDC (Dreyfus et al., 2007) (dark green: raw data; light green: 1 kyr re-sampled, filtered in the range 15–100 kyrs). The corresponding Y-axis is reversed.
- Precession (purple) and eccentricity (black)

The dashed vertical lines depict time periods when the peak to peak correspondence between $\delta O_2/N_2$ and insolation is difficult to identify. The time periods highlighted in yellow correspond to significant changes in the two time delays ($\delta O_2/N_2$ vs. nsolation and $\delta^{18}O_{atm}$ vs. precession).

CPD
7, 2217–2259, 2011

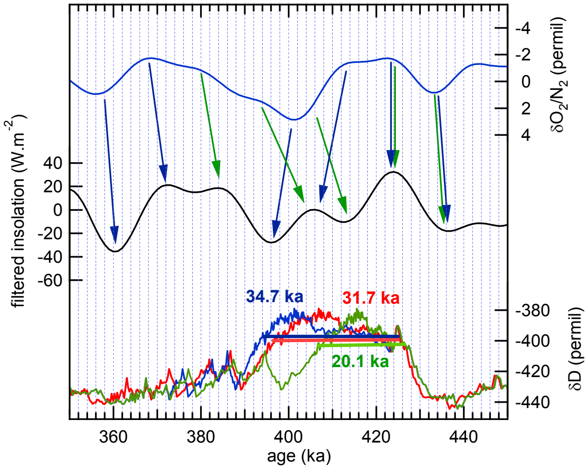

Fig. 8. Possible constraints on the duration of MIS 11 from the correspondence between $\delta O_2/N_2$ and 75° S 21 December insolation. To constrain the minimum/maximum duration of MIS 11 consistent with this orbital tuning method, we propose two extreme alignments of the minima and maxima of the $\delta O_2/N_2$ record with the maxima and minima of the insolation curves (see green/blue arrows). From top to bottom:

- Filtered (15–100 kyrs) $\delta O_2/N_2$ record (gas loss correction 2)
- Normalized 21 December insolation at 75° S
- δD record (Jouzel et al., 2007) on the original EDC3 age scale (red) and on two extreme age scales obtained by tuning $\delta O_2/N_2$ variations on the insolation curve in a subjective way depicted by the green/blue arrows.

The horizontal bars on the bottom panel with indicate the length of the MIS 11 interglacial on the EDC3 age scale (red) (using a −403 ‰ δD threshold to define the start and end of interglacials), the minimal length of the MIS 11 interglacial as deduced from the $\delta O_2/N_2$ record (green) and the maximal length of the MIS 11 interglacial as deduced from the $\delta O_2/N_2$ record (blue).

CPD
7, 2217–2259, 2011

Towards orbital dating of the EPICA Dome C ice core

A. Landais et al.